DE GRUYTER Nanotechnology Reviews 2020; 9: 922–933

Research Article

Qing'e Wang, Kai Zheng, Huanan Yu*, Luwei Zhao, Xuan Zhu, and Junqian Zhang

# Laboratory experiment on the nano-$TiO_2$ photocatalytic degradation effect of road surface oil pollution

https://doi.org/10.1515/ntrev-2020-0072
received August 27, 2020; accepted September 16, 2020

**Abstract:** Oil leak from vehicles is one of the most common pollution types of the road. The spilled oil could be retained on the surface and spread in the air voids of the road, which results in a decrease in the friction coefficient of the road, affects driving safety, and causes damage to pavement materials over time. Photocatalytic degradation through nano-$TiO_2$ is a safe, long-lasting, and sustainable technology among the many methods for treating oil contamination on road surfaces. In this study, the nano-$TiO_2$ photocatalytic degradation effect of road surface oil pollution was evaluated through the lab experiment. First, a glass dish was used as a substrate to determine the basic working condition of the test; then, a test method considering the impact of different oil erosion degrees was proposed to eliminate the effect of oil erosion on asphalt pavement and leakage on cement pavement, which led to the development of a lab test method for the nano-$TiO_2$ photocatalytic degradation effect of oil pollution on different road surfaces.

*** Corresponding author: Huanan Yu,** Department of Road Engineering, National Engineering Laboratory of Highway Maintenance Technology, School of Traffic and Transportation Engineering, Changsha University of Science & Technology, Changsha, 410114, Hunan, China, e-mail: huanan.yu@csust.edu.cn
**Qing'e Wang:** Department of Engineering Management, School of Civil Engineering, Central South University, Changsha, 410000, Hunan, China, e-mail: wqecsu@csu.edu.cn
**Kai Zheng:** China Railway 14th Bureau Group Co. Ltd, Shandong, China, e-mail: 1055146556@qq.com
**Luwei Zhao:** Department of Engineering Management, School of Civil Engineering, Central South University, Changsha, 410000, Hunan, China, e-mail: luweizhao@csu.edu.cn
**Xuan Zhu:** Department of Road Engineering, School of Traffic and Transportation Engineering, Changsha University of Science & Technology, Changsha, 410114, China, e-mail: zhuxuan@stu.csust.edu.cn
**Junqian Zhang:** Department of Civil Engineering, School of Civil Engineering, Central South University, Changsha, 410000, Hunan, China, e-mail: jqstark@163.com
ORCID: Huanan Yu 0000-0001-9491-6383

**Keywords:** nano-$TiO_2$, photocatalytic degradation, road surface, oil pollutions, testing method

## 1 Introduction

With the rapid development of transportation in China, the environmental problems associated with road traffic operation cannot be ignored [1,2]. In recent years, frequent incidents of oil pollution occurring in traffic operation have caused serious impacts on roads and the surrounding environment, and the negative impact of traffic operations on the environment has become increasingly prominent [3].

The main source of road surface oil pollution is the leakage of motor vehicle fuels (gasoline and diesel) and lubricants. Spilled oil will remain on the surface of the road and spread in the air voids of the pavement, which could result in a decrease in the friction coefficient of the road, affect driving safety, and cause damage to pavement materials over time, and thus reduce the service life of the road [4]. At the same time, on the road surface polluted by the oil spill, the road runoff formed by rain erosion will cause secondary pollution of the surrounding soil and water.

The photocatalytic degradation is a safe, long-lasting, and sustainable technology in the treatment of air pollutions [5–9] and road surface oils [10,11]. The basic mechanism is that photocatalytic materials will induce photo-oxidation–reduction reactions under the action of light. When it is exposed to high energy light, it generates highly reactive electron–hole pairs on the surface, which will interact with dissolved oxygen and water molecules adsorbed on the surface of the material and eventually oxidize and degrade the organic matter into inorganic substances such as $CO_2$ and $H_2O$, as shown in Figure 1. The reaction mechanism contains the following reaction formula (1) to formula (9) [12,13].

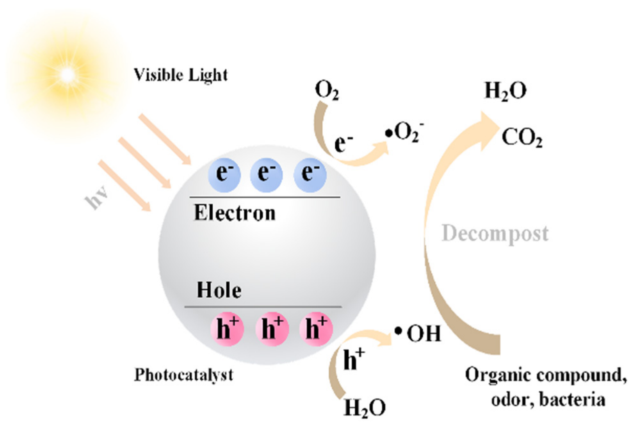


**Figure 1:** Diagram of photocatalytic degradation mechanism.

$$\text{photocatalyst} + hv \rightarrow h^+ + e^- \quad (1)$$

$$h^+ + H_2\,O \rightarrow OH + H^+ \quad (2)$$

$$e^- + O_2 \rightarrow O_2^- \rightarrow \ ^{\cdot}HO_2 \quad (3)$$

$$2^{\cdot}HO_2 \rightarrow O_2 + H_2O_2 \quad (4)$$

$$O_2^- + H_2O_2 \rightarrow \ ^{\cdot}OH + OH^- + O_2 \quad (5)$$

$$H_2O_2 + e^- \rightarrow \ ^{\cdot}OH + OH^- \quad (6)$$

$$OH^- + h^+ \rightarrow \ ^{\cdot}OH \quad (7)$$

$$OH + \text{Organ} \rightarrow HO_2 + CO_2. \quad (8)$$

The aforementioned reaction process can be summarized as formula (9):

$$\text{Organ} + O_2 \xrightarrow{hv+\text{photocatalyst}} CO_2 + H_2O. \quad (9)$$

A large number of research studies have shown that photocatalysts loaded onto suitable carriers can be effectively applied for the treatment of oil pollution. For example, Heller [14] conducted an outdoor experiment in which 100 µm diameter hollow glass spheres were loaded with $TiO_2$ and made to float on the water surface for oil pollution degradation. Berry and Mueller [15] used $TiO_2$ powder as the photocatalytic material and adhered it to wood chips with epoxy resin, and the test result showed that it could effectively degrade petroleum pollutants on the water surface. Zhang et al. [16] also evaluated nano-$TiO_2$ in water treatment. King et al. [17] and Yang et al. [18] found that the photocatalytic technology was useful in the degradation of the oil in the Deepwater Horizon spill accident.

Ziolli and Jardim [19] used photocatalytic technology to analyze and determine the degradation of crude oil with nano-$TiO_2$. In this experimental study, nano-$TiO_2$ was used as a photocatalyst under a UV light source, and the result shows that the degradation rate of crude oil could reach more than 90% after 24 h of UV irradiation. Kim et al. [20] investigated the degradation of petroleum hydrocarbons by the $TiO_2$ suspension system. In 2002, a 7,000 $m^2$ environmentally friendly pavement was constructed in Milan, Italy, in which the photocatalyst was mixed with cement slurry in a certain proportion and then coated on the surface of the pavement, and the gas test results showed that the degradation rate of the photocatalyst on the pavement was still high for nitrogen oxides after long-term use [21,22].

Research related to the application of photocatalytic materials on pavements is also becoming an important aspect of environmentally friendly pavement construction. Researchers [23–25] analyzed the degradation properties of $TiO_2$-doped pavement material on $NO_X$ and found that nano-$TiO_2$ did not adversely affect the physical properties of pavement materials before and after incorporation. Chen and Liu [26] prepared nano-$TiO_2$-containing specimens by infiltration technique based on the porous characteristics of concrete and investigated the effects of surface friction, humidity and light intensity on the efficiency of $NO_X$ decomposition. Based on vehicle emissions of decontamination by using nanometer $TiO_2$ of photocatalysis method, Ai and Chen [27] had optimized the nano-$TiO_2$ content, and surfactant utilized the permeability technology to make concrete with nano-$TiO_2$. Chen et al. [28] examined the potential use of heterogeneous photocatalysis as an innovative oxidation technology and found that this technology can reduce the damaging effects of vehicle emissions by using nitrogen-doped (N-doped) $TiO_2$ as a photocatalyst coated on the asphalt road surface. The experimental results showed that an N-doped $TiO_2$ asphalt road material has a higher activity compared with a pure $TiO_2$ asphalt road material under visible light irradiation. Tseng and Kuo [29] found that the carbonaceous species on the $TiO_2$ surface plays an important role in the visible-light absorption and photocatalytic degradation rates for $NO_X$ and methyl orange through photoluminescence, Raman, UV-vis, infrared, and X-ray photoelectron spectroscopies. Lei et al. [30] evaluated the ball milling process on the photocatalytic performance of CdS/$TiO_2$ composite through X-ray diffraction and UV-Vis diffuse reflectance spectroscopy methods. Zhang et al. [31] and Ossai and Raghavan [32] evaluated the properties of nano-modified materials for cement-based materials.

From the above literature review, it can be seen that scholars have achieved much progress in the use of $TiO_2$ for the treatment of oil pollution on water surfaces and the construction of environmentally friendly roads. However, in the current road engineering, there is a lack of systematic studies on the quantitative effects and influence laws of $TiO_2$ in degrading oil pollution on road surfaces. Most of the applied research studies on the treatment of oil pollutants by $TiO_2$, were focused on the treatment of water surface oil pollution, while the studies on the effects of photocatalytic degradation of oil pollution on road surfaces and the corresponding test methods and evaluation indexes for cement concrete or asphalt pavements are still relatively few. Besides, many researchers have found that the nanoparticles can potentially improve the rutting and cracking resistance of asphalt mixtures, which make the application of $TiO_2$ on the asphalt pavement to be more applicable [33–39].

The nano-$TiO_2$ particles are in the dimension of 100 nm or less, which makes the nanoparticles have a greater surface area and let them be more reactive with oil spills [40,41]. In this study, a lab test method for photocatalytic degradation of the effects of road surface oil pollution was proposed to address the aforementioned problems. The glassware was used as a substrate to initially explore the basic working condition parameters, and then asphalt pavement and cement concrete were used as substrates to simulate the oil degradation effect of the two types of the pavement surface.

# 2 Research methodology

Taking the oxidation ability, chemical stability and economics of various photocatalytic materials into consideration, nano titanium dioxide (nano-$TiO_2$) was selected as the test substrate because of the good photocatalytic performance, stable properties and wide application range. The nano-$TiO_2$ was applied on different substrates (simulating different pavement surfaces) by spraying and external penetration methods. Accordingly, a lab test procedure for photocatalytic degradation of oil on the road surface was proposed, and a simulation test method for photocatalytic degradation of oil on asphalt pavement and the concrete road surface was developed based on the optimization of the test conditions and the sensitivity analysis of the test parameters.

## 2.1 Test process design

For roads with a high risk of oil leakage and sensitive environmental impact, it is important to apply the protective nano-$TiO_2$ coating on the road surface to reduce the adverse effects of road surface oil pollution. Therefore, in this study, the test procedure was designed to analyze the effect of nano-$TiO_2$ photocatalytic degradation of road surface oil pollution, as shown in Figure 2.

The nano-$TiO_2$ photocatalytic degradation test of roadway oil stains was conducted in an environmental simulation system designed in house, which consisted of a light device and a temperature control device [42]. The light illumination device uses a UV-LED light source with a wavelength of 365 nm, including a controller and an irradiation head; the controller can adjust the UV output power of the light illumination device to adjust the light intensity within the range of 0–150 W/m$^2$. The illumination device is able to meet the requirements of simulating a variety of UV irradiation intensities in the test process.

In this study, the petroleum concentration and COD (Chemical Oxygen Demand) values were selected as the evaluation indicators. The samples collected were assessed for water quality, the COD, and petroleum concentration tests, and the main test instruments are shown in Table 1, and the corresponding chemical

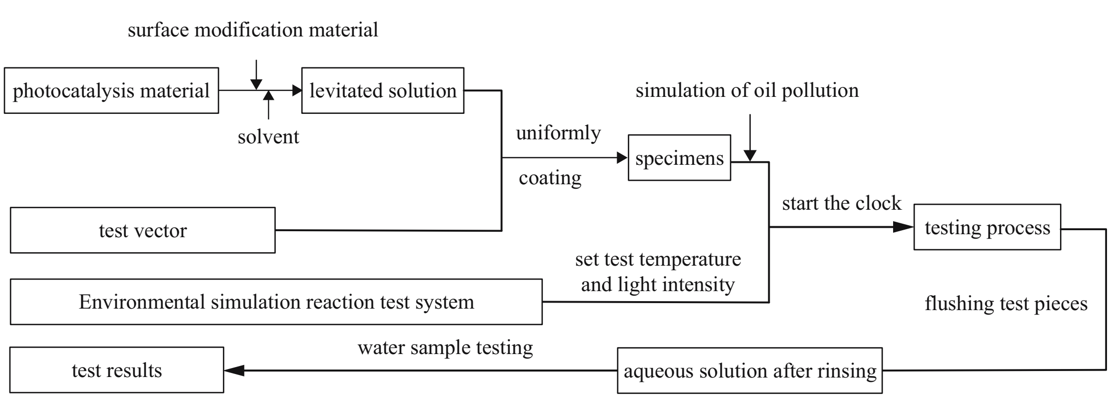


**Figure 2:** Test flow diagram.

Table 1: Indicators and methods for water quality testing

| Serial number | Test items | Test method | Testing equipment |
|---|---|---|---|
| 1 | COD | GB11914-89 | GDYS-201M (multiparameter water quality analyzer) |
| 2 | Petroleum | SL93.2-94 | MAI-50G (infrared oil detector) |

Table 2: Main technical parameters of nano-$TiO_2$

| Appearance | Crystallographic structure | Water content | Average particle size (nm) | Specific surface area ($m^2/g$) | Purity |
|---|---|---|---|---|---|
| White powder | Anatase | ≤0.5% | 20 | 50–100 | ≥99.8% |

Note: the water content is the percentage of dry weight loss after 2 h at 105°C.

Table 3: Main technical parameters of silane coupling agent

| Density ($g/cm^3$) | Refractive index | Boiling point (°C) | Characteristics |
|---|---|---|---|
| 0.949 | 1.423 | 213–216 | Colorless to light yellow transparent liquid |

reagents were stored according to the national sample storage standard (GB12997-91).

The degradation rate index was defined and used for the effect of photocatalytic pavement oil pollution, which was calculated by the following formula (10):

$$\text{Degradation rate (\%)} = \frac{C_0 - C_1}{C_0} \times 100\%, \qquad (10)$$

where $C_0$ is the contaminant concentration in water without photocatalysis (mg/L) and $C_1$ is the contaminant concentration in water under photocatalytic conditions (mg/L).

## 2.2 Test materials

### 2.2.1 Nano-$TiO_2$ technical parameters

In this study, the commercially available VK-TG01 nano-$TiO_2$ was chosen as the photocatalytic substrate, and its main technical parameters are shown in Table 2.

Nanomaterials are prone to spontaneous agglomeration during transportation and storage and transformed into secondary particles with large particle size, which may lead to a significant decrease in the photocatalytic activity of the material. Therefore, it is necessary to perform surface modification to effectively prevent interparticle agglomeration and improve their photocatalytic activity.

### 2.2.2 Other materials and technical parameters

In addition to the nano-$TiO_2$, the other test materials involved mainly include the following:

#### 2.2.2.1 Surface modifiers

The surface modifiers can effectively prevent agglomeration between particles and improve the photocatalytic activity of the nano-$TiO_2$. The silane coupling agent was chosen as the surface modifier of the material in the test, and its main technical parameters are shown in Table 3.

#### 2.2.2.2 Deionized water

The deionized water can be used as a solvent to prepare the test material and to rinse the residual oil of the specimen in the test. The main technical parameters of the selected deionized water are shown in Table 4.

#### 2.2.2.3 Carbon tetrachloride

The carbon tetrachloride selected in this study is an environmentally friendly reagent used in conjunction with the infrared oil detector, and its main technical parameters are shown in Table 5.

Table 4: Main technical parameters of deionized water

| Conductivity (μS/cm) | 1 μm particle number (units/mL) | Bacteria number (units/mL) | Characteristics |
|---|---|---|---|
| ≤2.0 | ≤500 | ≤100 | Colorless Tasteless |

Table 5: Main technical parameters of carbon tetrachloride ($CCl_4$)

| Content | Moisture | Density (20°C, g/mL) | Evaporation residue | Acidity ($H^+$, mmol/100 g) | Characteristics |
|---|---|---|---|---|---|
| ≥99.5% | ≤0.02% | 1.592–1.598 | ≤0.001% | ≤0.005 | Colorless transparent |

Table 6: Main technical parameters of hydrochloric acid

| Content (HCl) | Scorched residue | Relative density (water = 1) | pH | Characteristics |
|---|---|---|---|---|
| 36–38% | ≤0.0005% | 1.2 | 2–3 | Colorless transparent |

Table 7: Main technical parameters of simulated oil stains

| SAE rating | Viscosity index | Pour point (°C) | Flashpoint (°C) | Density (15°C, kg/mL) |
|---|---|---|---|---|
| 20W-40 | 116 | −27 | 223 | 0.89 |

Table 8: Main technical parameters of anhydrous sodium sulfate

| Content ($Na_2SO_4$) | Scorched residue | Relative density ($g/cm^3$) | pH (25°C, 50 g/L) | Characteristics |
|---|---|---|---|---|
| ≥99.0% | ≤0.2% | 2.68 | 5.0–8.0 | Colorless transparent crystal |

#### 2.2.2.4 Hydrochloric acid

The hydrochloric acid was mainly used to acidify the collected aqueous solution, and the main technical parameters of the analytically pure hydrochloric acid used in this test are shown in Table 6.

#### 2.2.2.5 Lubricants

Since the lubricant spilled by motor vehicles is one of the main sources of oil stains on the road, a commercial lubricant was chosen to simulate oil stains in this test, and its main technical parameters are shown in Table 7.

#### 2.2.2.6 Anhydrous sodium sulfate

The anhydrous sodium sulfate was mainly used for the dewatering of carbon tetrachloride extraction solution in the test, and its main technical parameters are shown in Table 8.

Table 9: Main technical parameters of sodium chloride

| Content (NaCl) | Loss on drying | Density ($g/cm^3$) | pH (25°C, 50 g/L) | Characteristics |
|---|---|---|---|---|
| ≥99.5% | ≤0.5% | 2.165 | 5.0–8.0 | Colorless crystal |

#### 2.2.2.7 Sodium chloride

The sodium chloride was mainly used to reduce the solubility of oil in water to facilitate extraction in the test, and its main technical parameters are shown in Table 9.

## 2.3 Investigation for optimizing working conditions of the test

The effect of the nano-$TiO_2$ photocatalytic degradation for the oil pollution is influenced by various conditions,

**Table 10:** Experimental schemes for working conditions optimization

| Evaluation parameters | | Reference group |
|---|---|---|
| Nano-$TiO_2$ usage ($g/m^2$) | 0, 4.4, 8.8, 13.3, 17.7, 22.1, 26.5, 31.0, 35.4, 39.8, 44.2 | Nano-$TiO_2$ usage is 4.4 $g/m^2$, 26.5 $g/m^2$ |
| Ambient temperature (°C) | 5, 15, 25, 35, 45 | Luminous intensity is 30 $W/m^2$ |
| Luminous intensity ($W/m^2$) | 0, 5, 10, 15, 20, 25, 30, 35, 40, 45 | Test temperature is 25°C |
| Response time (h) | 0.25, 0.5, 0.75, 1, 1.25, 1.5, 2, 2.5, 3, 4, 6, 8 | Response time is 3 h |

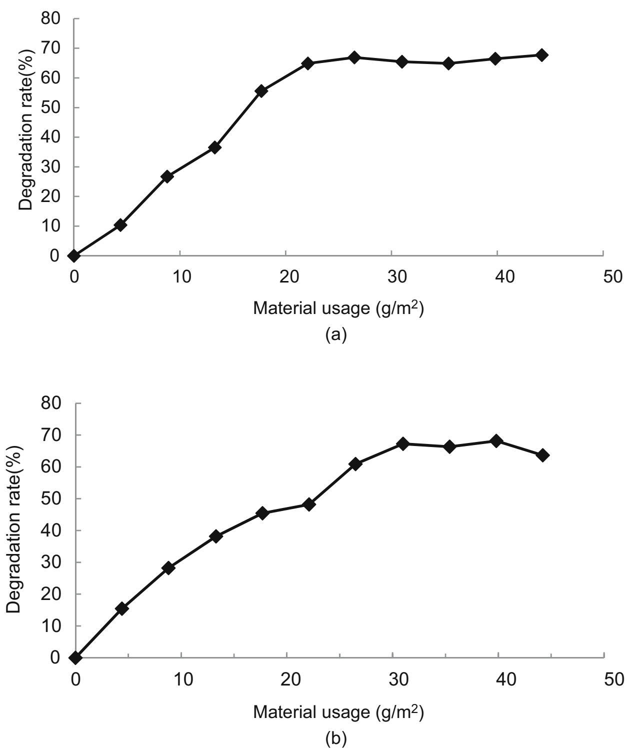


**Figure 3:** Degradation rate test results for different amounts of photocatalytic materials, (a) petroleum, (b) COD.

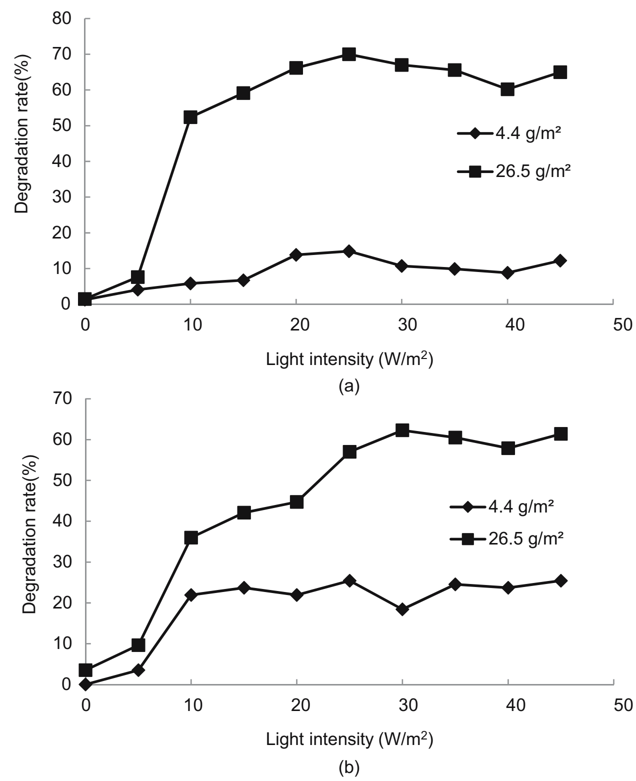


**Figure 4:** Test results of degradation rates under different light intensities, (a) petroleum, (b) COD.

such as road surface condition, the amount of oil pollution/nano-$TiO_2$ and its ratio, ambient temperature, light intensity, and light time [43]. Therefore, the sensitivity analysis of the relevant parameters was carried out in this experimental study.

Different road surface conditions have different degrees of dissolution or leakage for oil pollution, which may affect the determination of the degradation effect for oil pollution. Therefore, in order to eliminate the influence of different road surface conditions, a 12 cm diameter glass dish substrate was used for the initial test.

In order to find the optimum test condition for the nano-$TiO_2$ usage, the ambient temperature, the luminous intensity and response time, 11 different levels of nano-$TiO_2$ amount, 5 different ambient temperatures, 10 levels of different luminous intensities and 12 different response time levels were evaluated; the evaluating levels of different conditions are shown in Table 10. The reference group indicated that those parameters were kept unchanged when other test conditions were changed to conduct the sensitivity test. The test results are shown in Figures 3–6.

### 2.3.1 Impact of nano-$TiO_2$ amount

To evaluate the effect of different nano-$TiO_2$ amounts on the degradation effect, a total of 11 groups of tests were conducted in this study as shown in Table 10. Among them, the test group with 0 $g/m^2$ of nano-$TiO_2$ was used as a blank control group. The corresponding results of the degradation rates of petroleum and COD from the experimental analysis are shown in Figure 3(a) and (b).

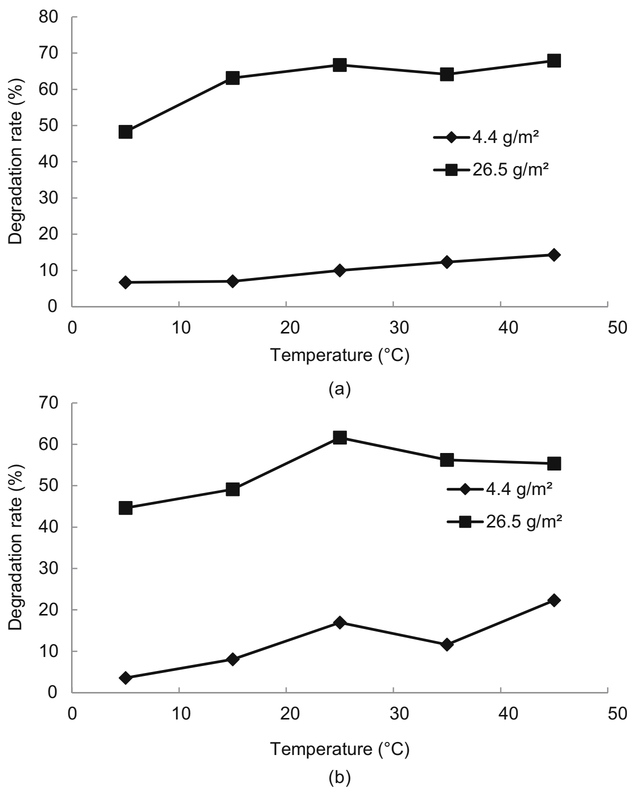


**Figure 5:** Test results of degradation rates under different ambient temperatures, (a) petroleum, (b) COD.

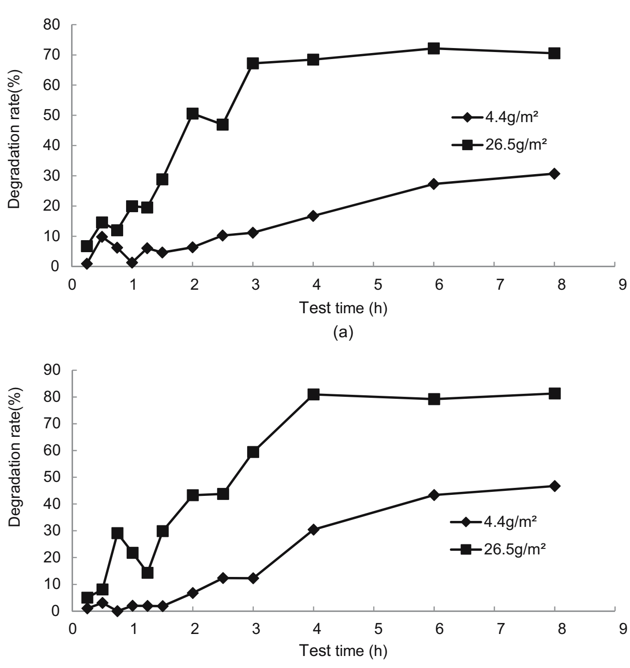


**Figure 6:** Test results of degradation rates under different reaction times, (a) petroleum, (b) COD.

It can be seen from Figure 3 that when the amount of nano-$TiO_2$ coated on the specimen was less than 22.1 g/m$^2$, the more the amount of nano-$TiO_2$, the better the degradation effect on simulated oil pollution; when the amount was more than 22.1 g/m$^2$, the degradation rate did not show any significant change. However, from the perspective of practical engineering application, the amount of nano-$TiO_2$ per unit area should not be too much, otherwise, it will affect the road performance such as the skid resistance [44].

### 2.3.2 Impact of lighting intensity

In order to evaluate the influence of different light intensities on the degradation effect, ten groups of different lighting intensity levels were conducted in this study, as shown in Table 10. Among them, the test group with a nano-$TiO_2$ dosage of 0 g/m$^2$ was used as a blank control group. The corresponding results of the degradation rates of petroleum and COD obtained from experimental analysis are shown in Figure 4(a) and (b).

It can be seen from Figure 4 that under conditions of different amounts of nano-$TiO_2$, the increase in illumination intensity has a significant effect on the simulated oil pollution degradation when the illumination intensity was within a lower certain range; when the illumination intensity was increased to a certain extent (for example, when the illumination intensity is 30 W/m$^2$ or above), the increase in illumination intensity had little effect on the degradation rate of simulated oil pollution.

### 2.3.3 Impact of test temperature

In order to evaluate the influence of different test temperatures on the degradation effect, five groups of tests were conducted in this study as shown in Table 10. Among them, the test group with a nano-$TiO_2$ dosage of 0 g/m$^2$ was used as a blank control group. The corresponding results of the degradation rates of petroleum and COD obtained from test analysis are shown in Figure 5(a) and (b).

Figure 5 shows that within a certain test temperature range, an increase in temperature can accelerate the photocatalytic degradation reaction, but when the temperature reached a certain level (up to 25°C in this test), the reaction temperature did not have a significant effect on the photocatalytic activity of material. The main reason is that most of the photocatalytic redox reactions are accompanied by endothermic or exothermic processes, which could cause certain influence of test temperature on the degradation effect, and the influence

**Table 11:** Results of Marshall tests under best bitumen aggregate ratio

| Asphalt content (%) | Density (g/cm$^3$) | Air voids VV (%) | Voids in mineral aggregate, VMA (%) | Voids filled with asphalt, VFA (%) | Marshall stability (KN) | Flow value (mm) |
|---|---|---|---|---|---|---|
| 5.2 | 2.431 | 5.0 | 16.1 | 67.2 | 16.3 | 2.73 |

is relatively obvious especially under the low temperature condition. However, the main factor affecting the effect of nano-$TiO_2$ photocatalytic degradation was still the electron–hole pairs excited by light, and the increase in temperature will not affect the number of electron–hole pairs that can be generated.

#### 2.3.4 Impact of reaction time

In order to evaluate the influence of different reaction times on the degradation effect, a total of 12 groups of tests were conducted in this study as shown in Table 10. Among them, the test group with 0 g/m$^2$ of nano-$TiO_2$ was used as a blank control group. The corresponding results of the degradation rates of petroleum and COD obtained from the experimental analysis are shown in Figure 6(a) and (b).

From Figure 6, it can be seen that the longer the reaction time, the better the degradation effect of the nano-$TiO_2$ on the simulated oil pollution under different dosages of nano-$TiO_2$; when a certain reaction critical time was reached, the photocatalytic degradation rate was stable; the result has shown that the critical time was reached faster with the increase in nano-$TiO_2$ amount. The result has shown that the critical reaction time was 3–6 h.

Therefore, based on the above analysis, 26.5 g/m$^2$ of simulated oil contamination per unit area was used (i.e., 0.3 g of oil contamination dropped onto the specimen surface), and 3,000 mL of water was used for rinsing the specimen. The luminous intensity was 30 W/m$^2$, the optimum test temperature was 25°C, and the selected response time was 3 h. The optimized test conditions are shown in Table 10.

## 3 Simulation test for photocatalytic degradation of oil asphalt pavement

When oil contamination occurs on road asphalt pavement, the conditions of field road surface were quite different from the previous simulation in glass dishes; the main reason was that the asphalt corrosion could increase the amount of pavement oil pollution during the test process, thus affecting the determination of degradation effect. Therefore, in the lab simulation study of asphalt pavement, the key point is how to determine the parameter $C_0$ in the aforementioned equation (10).

### 3.1 Preparation of basal specimens and coatings

In this test, the styrene butadiene styrene modified asphalt with strong resistance to oil corrosion was used [45,46]. The asphalt mixture was designed as dense-graded asphalt mixture AC-13C, and the aggregate of limestone material was used. The results of the specimen tests are shown in Table 11.

Rutting plate specimens were compacted according to the national standard, and the specimens were cut into 10 cm × 10 cm squares after it was formed, and the surface of the specimens was used as a substrate preparing for coating [47,48].

### 3.2 Treatment and analysis of asphalt pavement erosion

The oil stains on asphalt pavement could cause corrosion and thus affect the oil photocatalytic degradation test result; therefore, how to deal with this problem and how to select the working conditions of the blank control group in the test is the key to the simulation test method of nano-$TiO_2$ photocatalytic degradation of oil pollution on asphalt pavement.

Degradation tests of the blank control group under different working conditions were carried out, and the petroleum and COD concentration at different times under an oil amount of 30 g/m$^2$ and a flushing water amount of 3,000 mL were compared, and the test result is shown in Figure 7. The working condition of T–G was the control group with a nano-$TiO_2$ coating of 0 g/m$^2$, a light intensity of 30 W/m$^2$, and a test temperature of 25°C on the glass

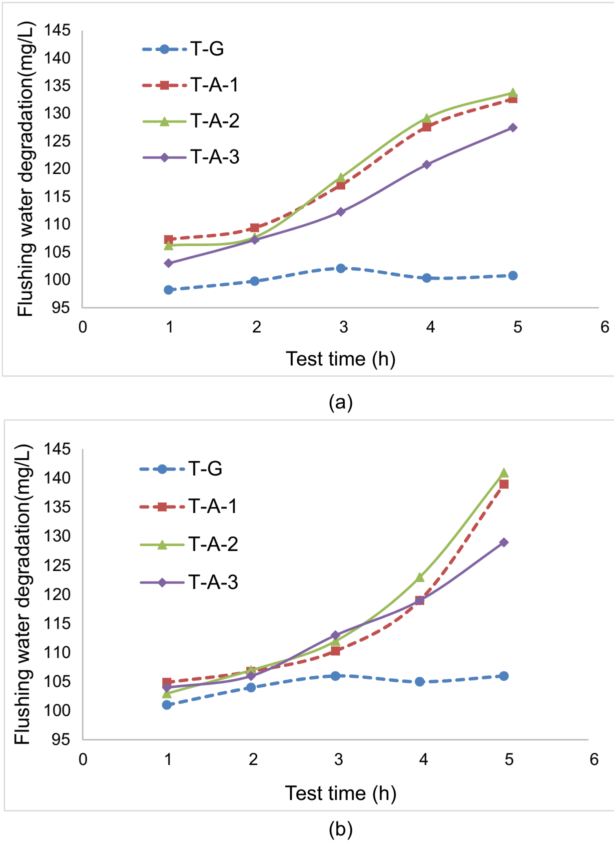


**Figure 7:** Test results of degradation test in the blank control group, (a) petroleum, (b) COD.

substrate; working condition of T-A-1 was the test with a nano-$TiO_2$ coating of 0 g/m$^2$, a light intensity of 30 W/m$^2$, and a test temperature of 25°C on the asphalt substrate; working condition of T-A-2 was the test with a nano-$TiO_2$ coating of 30 W/m$^2$, a light intensity of 30 W/m$^2$, and a test temperature of 25°C on the asphalt substrate; and working condition of T-A-3 was the test with a nano-$TiO_2$ coating dosage of 5 g/m$^2$, a light intensity of 0 W/m$^2$, and a test temperature of 25°C on the asphalt mixture base.

It can be seen from Figure 7(a) and (b) that the phenomenon for asphalt corrosion is obvious compared with the glass dish substrate under the action of the oil. Therefore, it is important to reasonably evaluate the corrosion in the photocatalytic degradation test of oil on asphalt pavement. The test results of the working condition T-A-1 and T-A-2 were close to each other, which indicated that the light intensity has little influence on the asphalt dissolution degree without photocatalytic materials. The coated material in working condition T-A-3 had a certain barrier effect on the contact between asphalt and oil, and the degree of asphalt dissolution was smaller than that in working conditions T-A-1 and T-A-2, which was closer to the actual pavement condition.

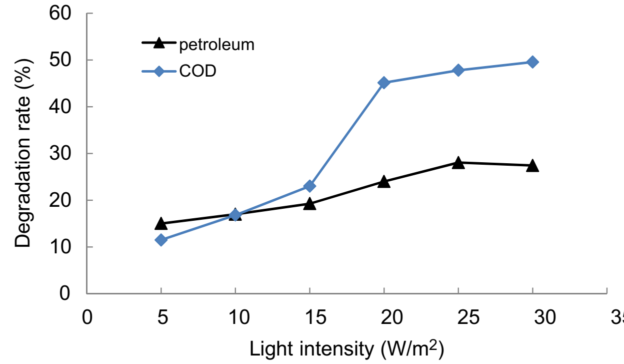


**Figure 8:** Oil degradation rate of asphalt pavement under different light intensities.

Therefore, when conducting the nano-$TiO_2$ photocatalytic degradation test of asphalt pavement oil pollution, the working condition T-A-3 could be referred to as the test conditions for the blank control group. The condition of T-A-3 was the nano-$TiO_2$ amount of 5 g/m$^2$, the test temperature of 25°C, and the reaction time of 3 h for test analysis; the impact of light intensity of 5, 10, 15, 20, 25, and 30 W/m$^2$; and the results of the degradation rates for petroleum and COD are shown in Figure 8.

## 4 Simulated method of photocatalytic degradation for oil pollution on cement pavement

In the case of oil pollution on cement pavement, the field conditions for road surface were quite different from the previous simulated working conditions of glass dish, and the cement concrete pavement has obvious oil leakage on its surface due to the porous properties, which could cause the oil leakage to be included in the degradation amount and could not reflect the actual degradation effect when the nano-$TiO_2$ photocatalytic degradation test was conducted. Therefore, the determination of the parameter $C_0$ in equation (10) was also a key consideration in the lab simulate study for cement pavements.

### 4.1 Preparations of substrates and coatings

The typical #42.5 Portland cement was used in this test; the limestone crushed stone with the particle size of

4.75–26.5 mm was chosen as the coarse aggregate with the water–cement ratio of 0.36, and natural river sand was used as the fine aggregate to prepare for the test specimens.

In the lab simulated test study of cement concrete pavements, cement concrete specimens with dimensions of 10 cm × 10 cm × 10 cm were prepared, and the nano-$TiO_2$ was loaded on their surfaces by external penetration for simulating cement concrete pavements coated with nano-$TiO_2$.

## 4.2 Treatment and analysis of the cement pavement oil leakage problems

The problem of oil leakage on cement pavements during degradation tests could affect the nano-$TiO_2$ photocatalytic degradation test result of the pavement oil pollution; therefore, how to deal with this problem and how to select the working conditions of the blank control group in the test were also key to the simulation for oil photocatalytic degradation on cement pavement.

The degradation test of the blank control group was carried out to compare the petroleum concentration and COD changes under the condition of 30 $g/m^2$ of oil amount, and the test result is shown in Figure 9. The base condition for working condition T-G was a glass dish substrate, a nano-$TiO_2$ coating dosage of 0 $g/m^2$, a light intensity of 30 $W/m^2$, a test temperature of 25°C; the base condition for working condition T-C-1 was a cement pavement substrate, a nano-$TiO_2$ coating dosage of 0 $g/m^2$, a light intensity of 30 $W/m^2$, a test temperature of 25°C; the base conditions for working conditions T-C-2 and T-C-3 were the same as those for working condition T-C-1, except that the initial oil contamination of the substrate under the two conditions was 60 and 90 $g/m^2$, respectively.

It can be seen from Figure 9(a) and (b) that compared with the glass dish substrate, the cement pavement substrate had a significant oil leakage phenomenon, which indicated that it should be reasonably considered the oil leakage when conducting the nano-$TiO_2$ photocatalytic degradation test of cement pavement oil pollution. The test results under working conditions of T-C-1, T-C-2, and T-C-3 showed that the cement concrete substrate had a saturation capacity of oil leakage from the pavement, and no further leakage could occur after the saturation capacity was reached.

During the oil pollution degradation of the cement pavement, the reduction in the amount of oil pollution comes from the amount of degradation and the amount of leakage. Therefore, during the nano-$TiO_2$ photocatalytic degradation test for the oil pollution of the cement pavement, the saturated leakage amount is deducted from the test, and the specimens are subjected to 3 h of leakage as a blank control group. The basic working condition is the nano-$TiO_2$ amount of 5 $g/m^2$; the light intensity of 5, 10, 15, 20, 25, 30, and 35 $W/m^2$; the test temperature of 25°C; and the reaction time of 3 h for the test analysis, and the results of degradation rates for the petroleum and COD are shown in Figure 10.

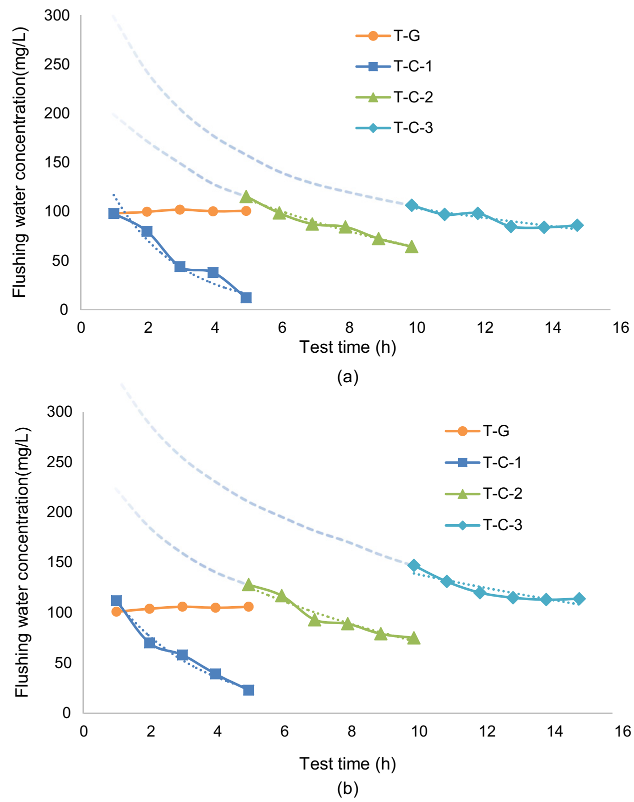


**Figure 9:** Test results of degradation test in the blank control group, (a) petroleum, (b) COD.

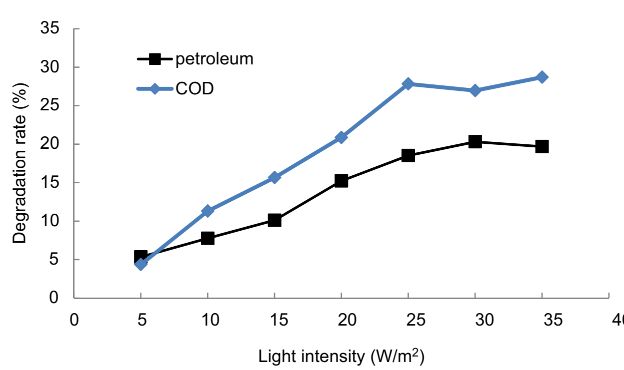


**Figure 10:** Degradation rate of oil on cement pavement at different light intensities.

## 5 Conclusions

In this study, aiming at the treatment of oil pollution for pavements in road operation, the lab testing and evaluation methods for the degradation of oil pollution from road surfaces through nano-$TiO_2$ were conducted, the following conclusions can be drawn:

(1) A lab test method for the determination of the effect of photocatalytic degradation for oil pollution on the road surface by nano-$TiO_2$ was proposed, and the standard working conditions of the test method were determined by optimizing the test conditions of ambient temperature, light intensity, and illumination time on the glass substrate.

(2) As the oil corrosion of asphalt greatly impacts the test result oil degradation on asphalt pavement, a test method was proposed in this research which is able to eliminate that by reasonably selecting the working conditions of the blank control group for the test.

(3) As the oil leakage greatly affects the photocatalytic degradation test result of the oil pollution on cement concrete pavement, a method was proposed to eliminate the oil leakage impact by reasonably selecting the working conditions of the blank and control group for the test.

**Conflict of interest:** The authors declare no conflict of interest regarding the publication of this paper.

## References


[1] He ZM, Xiang D, Liu YX, Gao QF, Bian HB. Deformation behavior of coarse-grained soil as an embankment filler under cyclic loading. Adv Civ Eng. 2020;3:1–13. doi: 10.1155/2020/4629105.

[2] Hasan MM, Rahman ASMA, Tarefder RA. Investigation of accuracy of pavement mechanistic empirical prediction performance by incorporating Level 1 inputs. J Traffic Transp Eng (Engl Ed). 2020;7(2):259–68.

[3] Wang QE, Zeng L, Chen HH, Qian GP. Research on Water-Environmental Emergency Management in Expressway Area. China Communications Press Co., Ltd; 2019.

[4] Plati C, Pomoni M, Georgouli K. Quantification of skid resistance seasonal variation in asphalt pavements. J Traffic Transp Eng (Engl Ed). 2020;7(2):237–48.

[5] Qian C, Zhao L, Fu D, Li L, Wang R. Photocatalytic oxidation of nitrogen oxides by nano-$TiO_2$ immobilised on road surface materials. J Chin Ceram Soc. 2005;33(4):422–7. doi: 10.1111/j.1744-7909.2005.00184.x.

[6] Kun R, Mogyorosi K, Dekany I. Synthesis and structural and photocatalytic properties of $TiO_2$/montmorillonite nanocomposites. Appl Clay Sci. 2006;32(1–2):99–110. doi: 10.1016/j.clay.2005.09.007.

[7] Carneiro JO, Azevedo S, Teixeira V, Fernandes F, Freitas E, Silva H, et al. Development of photocatalytic asphalt mixtures by the deposition and volumetric incorporation of $TiO_2$ nanoparticles. Constr Build Mater. 2013;38:594–601. doi: 10.1016/j.conbuildmat.2012.09.005.

[8] Liang H, Wang Z, Liao L, Chen L, Li Z, Feng J. High performance photocatalysts: montmorillonite supported-nano $TiO_2$ composites. Opt - Int J Light Electron Opt. 2017;136:44–51. doi: 10.1016/j.ijleo.2017.02.018.

[9] Yu HN, Dai W, Qian GP, Gong XB, Zhou DY, Li X, et al. The $NO_x$ degradation performance of Nano-$TiO_2$ coating for asphalt pavement. Nanomaterials. 2020;10(5):897. doi: 10.3390/nano10050897.

[10] Khitab A, Ahmad S, Munir MJ, Kazmi SMS, Arshad T, Khushnood RA. Synthesis and applications of nano titania particles: a review. Rev Adv Mater Sci. 2018;53(1):90–105. doi: 10.1515/rams-2018-0007.

[11] Gannavarapu KP, Thakkar M, Veerapaga S, Wei L, Dandamudi RB, Mitra S. Novel diatom-$FeO_x$ composite as highly active catalyst in photodegradation of Rhodamine-6G. Nanotechnol Rev. 2018;7(3):247–55. doi: 10.1515/ntrev-2017-0218.

[12] Liu R, Xue XX, Yang H, Jiang T, Dong XW. Progress on the application of photocatalysis oxidation in environmental protection. Energy Environ Prot. 2004;18(4):5–8. doi: 10.3969/j.issn.1006-8759.2004.04.002.

[13] Yu BC, Wu HT, Zhang WZ. Application of nano-photocatalysts in environmental protection. Pet Technol. 2005;4(5):491–5. doi: 10.3321/j.issn:1000-8144.2005.05.020.

[14] Heller A. Abstracts of the First International Conference on $TiO_2$ Photocatalytic Purification and Treatment of Water and Air. London, Ontario, Canada; 1992. 17.

[15] Berry RJ, Mueller MR. Photocatalytic decomposition of crude oils licks using $TiO_2$ on a floating substrate. Microchem J. 1994;50(1):28–32. doi: 10.1006/mchj.1994.1054.

[16] Zhang P, Ling YF, Wang J, Shi Y. Bending resistance of PVA fiber reinforced cementitious composites containing nano-$SiO_2$. Nanotechnol Rev. 2019;8(1):690–8. doi: 10.1515/ntrev-2019-0060.

[17] King SM, Leaf PA, Olson AC, Ray PZ, Tarr MA. Photolytic and photocatalytic degradation of surface oil from the deepwater horizon spill. Chemosphere. 2014;95:415–22. doi: 10.1016/j.chemosphere.2013.09.060.

[18] Yang ZY, Hollebone BP, Zhang G, Brown CE, Yang C, Lambert P, et al. Chemical fate of photodegraded diluted bitumen in seawater. Int Oil Spill Conf Proc. 2017;2017(1):2286–305. doi: 10.7901/2169-3358-2017.1.2286.

[19] Ziolli RL, Jardim WF. Photochemical transformations of water-soluble fraction (WSF) of crude oil in marine waters. A comparison between photolysis and accelerated degradation with $TiO_2$ using GC-MS and UVF. J Photochem Photobiol A Chem. 2003;155:243–52. doi: 10.1016/S1010-6030(02)00397-0.

[20] Kim LH, Zoh KD, Cho H. Solar photocatalytic degradation of groundwater contaminated with petroleum hydrocarbons. Environ Prog. 2006;25(2):99–109. doi: 10.1002/ep.10124.

[21] Alexandre V. $TiO_2$ Reactivation in photocatalytic destruction of gaseous diethyl sulfide in a coil reactor. Appl Catal B. 2003;44(1):25–40. doi: 10.1016/s0926-3373(03)00007-9.

[22] Muggli DS, Falconer JL. Role of lattice oxygen in photocatalytic oxidation on $TiO_2$. J Catal. 2000;191(2):318–25. doi: 10.1006/jcat.2000.2821.

[23] Typek J, Guskos N, Zolnierkiewicz G, Pilarska M, Guskos A, Kusiak-Nejman E, et al. Magnetic properties of $TiO_2$/graphitic carbon nanocomposites. Rev Adv Mater Sci. 2019;58(1):107–22. doi: 10.1515/rams-2019-0009.

[24] Skiba NV. Mechanism of stress-driven grain boundary migration in nanotwinned materials. Rev Adv Mater Sci. 2018;55(1):21–5. doi: 10.1515/rams-2018-0024.

[25] Hassan M, Mohammad L, Cooper S, Dylla H. Evaluation of nano-titanium dioxide additive on asphalt binder aging properties. Transp Res Rec. 2011;2207:11–5. doi: 10.3141/2207-02.

[26] Chen M, Liu Y. $NO_X$ removal from vehicle emissions by functionality surface of asphalt road. J Hazard Mater. 2010;174:375–9. doi: 10.1016/j.jhazmat.2009.09.062.

[27] Ai XF, Chen M. The decontamination of vehicle emissions $NO_x$ through functionality surface of concrete road. Adv Mater Res. 2011;255–60:2930–3. doi: 10.4028/www.scientific.net/AMR.255-260.2930.

[28] Chen M, Baglee D, Chu JW, Du DF, Guo XR. Photocatalytic oxidation of $NO_x$ under visible light on asphalt-pavement surface. J Mater Civ Eng. 2017;29(9):1. ISSN 0899-1561. doi: 10.1061/(ASCE)MT.1943-5533.0001972.

[29] Tseng YH, Kuo CH. Photocatalytic degradation of dye and $NO_x$ using visible-light-responsive carbon-containing $TiO_2$. Catal Today. 2011;174(1):114–20. doi: 10.1016/j.cattod.2011.02.011.

[30] Lei M, Chen Z, Lu H, Yu K. Recent progress in shape memory polymer composites: methods, properties, applications and prospects. Nanotechnol Rev. 2019;8(1):327–51. doi: 10.1515/ntrev-2019-0031.

[31] Zhang P, Li Q, Wang J, Shi Y, Ling Y. Effect of PVA fiber on durability of cementitious composite containing nano-$SiO_2$. Nanotechnol Rev. 2019;8(1):116–27. doi: 10.1515/ntrev-2019-0011.

[32] Ossai CI, Raghavan N. Nanostructure and nanomaterial characterization, growth mechanisms, and applications. Nanotechnol Rev. 2017;7(2):209–31. doi: 10.1515/ntrev-2017-0156.

[33] Dehouche N, Kaci M, Mouillet V. The effects of mixing rate on morphology and physical properties of bitumen/organo-modified montmorillonite nanocomposites. Constr Build Mater. 2016;114:76–86. doi: 10.1016/j.conbuildmat.2016.03.151.

[34] Ghasemi M, Marandi SM, Tahmooresi M, Kamali RJ, Mousavian RT. Modification of stone matrix asphalt with nano-$SiO_2$. J Basic Appl Sci Res. 2012;2(2):1338–44.

[35] Goli A, Ziari H, Amini A. Influence of carbon nanotubes on performance properties and storage stability of SBS modified asphalt binders. J Mater Civ Eng. 2017;29(8):04017070. doi: 10.1061/(asce)mt.1943-5533.0001910.

[36] You Z, Mills-Beale J, Foley JM, Roy S, Goh SW. Nanoclay-modified asphalt materials: preparation and characterization. Constr Build Mater. 2011;25(2):1072–8. doi: 10.1016/j.conbuildmat.2010.06.070.

[37] Shi X, Goh SW, Akin M, Stevens S, You Z. Exploring the interactions of chloride deicer solutions with nanomodified and micromodified asphalt mixtures using artificial neural networks. J Mater Civ Eng. 2012;24(7):805–15. doi: 10.1061/(ASCE)MT.1943-5533.0000452.

[38] Qian G, Yu H, Gong X, Zhao L. Impact of nano-$TiO_2$ on the $NO_2$ degradation and rheological performance of asphalt pavement. Constr Build Mater. 2019;218:53–63. doi: 10.1016/j.conbuildmat.2019.05.075.

[39] Yousefian R, Emadoddin E, Baharnezhad S Manufacturing of the aluminum metal-matrix composite reinforced with micro- and nanoparticles of $TiO_2$ through accumulative roll bonding process (Arb). Rev Adv Mater Sci. 2018;55(1):1–11. doi: 10.1515/rams-2018-0022.

[40] Krylova KA, Babicheva RI, Zhou K, Bubenchikov AM, Ekomasov EG, Dmitriev SV. The effect of crystallographic orientation on the deformation mechanisms of nial nanofilms under tension. Rev Adv Mater Sci. 2018;57(1):26–34. doi: 10.1515/rams-2018-0044.

[41] Zhang Z, An Y. Nanotechnology for the oil and gas industry – an overview of recent progress. Nanotechnol Rev. 2018;7(4):341–53. doi: 10.1515/ntrev-2018-0061.

[42] Qian GP, Huang SX, Qin ZB, Li YQ, Ju SJ, Su ZH, et al. (2015). Gas-Solid Phase Photocatalytic Reaction Effect Detection Device and Method with Controllable Variationof Influence Factors. Patent 2013 1 0017395.1.2015-05-20.

[43] Qian GP, Zheng K, Zheng W, Zuo RF. Experimental study on photocatalytic degradation of road surface oil pollution. Environ Sci Technol. 2015;38:172–6.

[44] Zhou D. The research on $NO_x$ degradation performance of asphalt pavement coating by nanometer-$TiO_2$. Hunan, China: Department of Road Engineering, Changsha University of Science and Technology; 2014.

[45] Wang J, Wang XP, Zheng HX, Li JS. Study on the influence of vehicle leakage on asphalt pavement and countermeasures. Technol Dev Enterp. 2010;29(15):87–9, 98. doi: CNKI:SUN:QYJK.0.2010-15-043.

[46] Vo HV, Park DW, Seo JW, Le THM. Effects of asphalt types and aging on healing performance of asphalt mixtures using induction heating method. J Traffic Transp Eng (Engl Ed). 2020;7(2):227–36. doi: 10.1016/j.jtte.2018.10.009.

[47] Technical Specification for Construction of Highway Asphalt Pavement. Beijing, Ministry of Transport of the People's Republic of China. JTG F40-2004, 2004.

[48] Ministry of Transport of the People's Republic of China. Standard Test Methods of Bitumen and Bituminous Mixtures for Highway Engineering: JTG E20-2011, 2011.